nature geoscience

ARTICLES

PUBLISHED ONLINE: 23 JANUARY 2017 | DOI: 10.1038/NGEO2883

Depletion and response of deep groundwater to climate-induced pumping variability

Tess A. Russo[1,2]* and Upmanu Lall[2,3]

Groundwater constitutes a critical component of our water resources. Widespread groundwater level declines have occurred in the USA over recent decades, including in regions not typically considered water stressed, such as areas of the Northwest and mid-Atlantic Coast. This loss of water storage reflects extraction rates that exceed natural recharge and capture. Here, we explore recent changes in the groundwater levels of deep aquifers from wells across the USA, and their relation to indices of interannual to decadal climate variability and to annual precipitation. We show that groundwater level changes correspond to selected global climate variations. Although climate-induced variations of deep aquifer natural recharge are expected to have multi-year time lags, we find that deep groundwater levels respond to climate over timescales of less than one year. In irrigated areas, the annual response to local precipitation in the deepest wells may reflect climate-induced pumping variability. An understanding of how the human response to drought through pumping leads to deep groundwater changes is critical to manage the impacts of interannual to decadal and longer climate variability on the nation's water resources.

Water use has increased by approximately 300% globally since the 1950s[1]. Many of the major aquifers in arid and semi-arid regions are experiencing rapid groundwater depletion[2]. In the USA, groundwater accounts for over 40% of water consumed for irrigation, livestock, and domestic water use (Supplementary Fig. 1)[3]. The percentage of irrigation demands met with groundwater rose significantly over the twentieth century, in many cases leading to extraction exceeding natural aquifer recharge rates[4]. In the US High Plains Aquifer, fossil groundwater is extracted for irrigation at nearly ten times the rate of recharge, resulting in the largest groundwater depletion in the country[5–7]. In locations that are not typically regarded as water stressed, groundwater may be used to make up the difference under drought conditions[8], leading to a potentially strong, asymmetric response to precipitation variability.

Shallow groundwater is present for a majority of the land surface, sustaining river baseflow and ecosystem functions[9]. Deeper groundwater serves as a valuable resource in regions lacking reliable access to surface water and often provides an essential buffer during dry seasons and droughts. Groundwater supplied for municipal, agricultural, or industrial purposes is drawn almost exclusively from wells >30 m in depth. Despite broad reliance on deep groundwater resources, measurements and assessments of groundwater availability are typically limited to individual basins, aquifers, or are skewed by the inclusion of shallow aquifers which are often not used for water supply.

Groundwater depths and trends

Groundwater level data for this study were obtained from the US Geological Survey[10]. Depth-to-water values were downloaded for 15,148 wells having at least 100 observations with records between 1940 and 2015 (Supplementary Fig. 2). Wells were classified by screen depth: S (0–30 m; $n = 6,974$), M (30–150 m; 5,707 wells), D (>150 m; 2,467 wells). Wells classified as M and D are herein referred to as 'deep'.

Recent average depth to groundwater varies regionally in deep (>30 m) wells across the USA (Fig. 1). Over 50% of the monitored deep wells have water tables or piezometric surfaces greater than 20 m below land surface. The deepest groundwater levels are typically found in arid and semi-arid agricultural regions, except for some parts of the humid southeast. Statistically significant water level declines are observed in parts of most major aquifers, especially in irrigated agricultural areas (Fig. 2). The Mississippi Embayment and North Atlantic coast aquifer systems have seen recent groundwater depletion[6,11] associated with dramatic growth in irrigated area[12]. These aquifers show declines that are comparable to the more frequently discussed water-stressed regions of the High Plains and western United States. Rising groundwater level trends were most notable in parts of the northern California Central Valley, southern Nevada, and the northern High Plains Aquifer (Fig. 2). Trends in the 3,441 shallow (S) wells (Fig. 2a) found to be significant ($p < 0.1$) were evenly split between rising (51%) and declining (49%), although a majority of all trends were near zero. Of the 5,743 deep (M and D) wells (Fig. 2b) with significant ($p < 0.1$) trends, 3,906 (68%) had declining trends and 1,837 (32%) had rising trends between 1940 and 2015. Shallow groundwater level increases and declines in deeper aquifer layers may appear to co-occur for adjacent wells screened in a multi-layered aquifer system.

Groundwater–climate connections

Correlations between groundwater levels and precipitation over multiple timescales can help assess aquifer vulnerability to climate change[13] and the indirect influence of pumping[14,15]. Correlations to multi-year or decadal climate patterns, such as the Pacific Decadal Oscillation (PDO) and El Niño Southern Oscillation (ENSO) have been observed in several aquifers[16–19]. Deep aquifers are often semi-confined, and hence an assessment of their response to climate must consider the attenuation of a time-varying recharge signal as it passes through the unsaturated zone, the upper water table aquifer[20,21] and intervening clay layers. This can lead to long recharge travel time. Groundwater response to climate varies with local geology[22], land use and land cover[23], and other factors affecting infiltration and recharge rates. Identifying groundwater–climate

[1]Department of Geosciences, and the Earth and Environmental Systems Institute, The Pennsylvania State University, 310 Deike Building, University Park, Pennsylvania 16802, USA. [2]Columbia Water Center, Columbia University, 500 W 120th Street, New York, New York 10027, USA. [3]Earth & Environmental Eng., Columbia University, 500 W 120th Street, New York, New York 10027, USA. *e-mail: russo@psu.edu

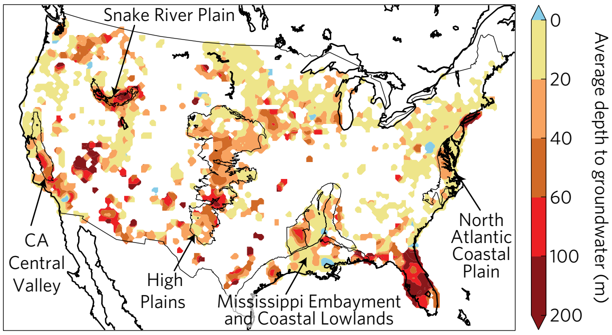

Figure 1 | Average groundwater level depth below ground surface for deep wells. White indicates no water level data; the scale is nonlinear. Five regional aquifer systems are outlined. CA, California.

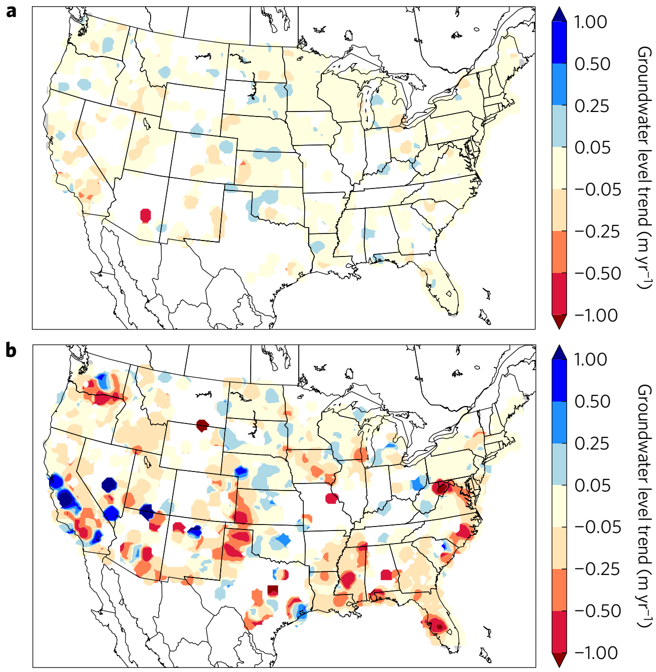

Figure 2 | Average groundwater level rate of change from wells with statistically significant trends ($p < 0.1$) observed between 1940 and 2015. **a**, Average groundwater level rate of change from shallow wells (depth <30 m). **b**, Average groundwater level rate of change from deep wells (depth >30 m). Negative trends (orange/red) indicate an average decline in groundwater level, and positive trends (blue) indicate a rise in groundwater level.

relations is further complicated by human use[14,24,25], making numerical modelling a valuable tool for estimating the impacts of irrigation on each major component of the hydrologic system[26].

Climate factors would nominally be expected to impact shallow, unconfined aquifers at sub-annual and annual timescales[27], and deep confined aquifers at interannual and longer timescales due to physical constraints on recharge signal travel time. Conversely, pumping has an immediate local impact on groundwater mass changes even in deep aquifers[28,29]. Multi-year climate cycles have had identifiable effects on groundwater levels, typically with the greatest correlation occurring when the groundwater lags the climate signal by more than 12 months, due to recharge travel and aquifer response time[24,30]. Two studies in the High Plains Aquifer (USA) investigated these relationships: one correlated regional pumping with precipitation and annual groundwater level change[15], whereas the other documented moderate correlations between groundwater level and pumping, with a less than one year lag, while correlations between groundwater level and annual precipitation had lags ranging from two to five years[24].

We use the multivariate ENSO index (MEI, 2–7 yr period), the North Atlantic Oscillation (NAO, 3–6 yr and 8–10 yr period), and the Pacific Decadal Oscillation (PDO, 15–30 yr period) index data from the National Oceanic and Atmospheric Administration[31]. Annual average precipitation data were obtained from Maurer and colleagues[32]. Kansas irrigation water-use data were obtained from the Kansas Government Information (KGI) Library[33].

A subset of 1,515 wells ($n_S = 652$; $n_M = 665$; $n_D = 198$) with nearly continuous groundwater level observations between 1963 and 2004 was selected for frequency analysis of groundwater and climate indices. The shorter study duration was chosen to maximize spatial coverage (Supplementary Fig. 3). Groundwater level records were clustered (Supplementary Fig. 4) and then compared to each climate index (Supplementary Fig. 5). Of the three climate indices analysed, the S and M groundwater records showed the greatest coherence to ENSO and PDO, which was also previously noted at the principal aquifer scale[16]. The deepest well depth category showed a stronger coherence with ENSO and NAO, rather than to PDO (Supplementary Table 1). Overall coherence with the ENSO, PDO and NAO increased with depth (Supplementary Table 2), suggesting strong groundwater–climate connections in the deep aquifers, a finding that is somewhat counter-intuitive considering the expected attenuation of the climate and recharge signal with depth and traversing confining layers.

Groundwater response to local precipitation and pumping

The response of groundwater levels to local precipitation variability was evaluated using a vector autoregression (VAR) impulse response function estimate applied to annual time series of the two variables. The model coefficients suggest that the groundwater response is largest within the first year of the precipitation change for all well depth categories (Fig. 3a). The time required for a recharge signal to travel from the land surface to the groundwater depends on aquifer properties and moisture content; for water tables more than a few metres from the surface or confined aquifers, it can take several years to respond to precipitation and groundwater recharge variability[22,24,30]. However, local groundwater responses to changes in water pumping are observable immediately. Wavelet analyses (see Supplementary Methods) show statistically significant interannual and decadal coherence between precipitation and deep groundwater changes, with precipitation typically leading groundwater change. The response may reflect rapid transmission of the recharge signal, or a deeper groundwater response may be due to shallow aquifer recharge causing pressure changes through well-connected deeper aquifers, whereas in deeper and less well-connected aquifers this signal is more likely due to climate-induced effects on groundwater demand and pumping.

We ascribe the near-synchronous response between precipitation and deep and/or confined aquifer systems to the human response to persistent drought and wet periods that accompany interannual climate variability. The strongest one-year groundwater response to precipitation appears to correspond with irrigated agricultural regions (Supplementary Fig. 1) in the western states, parts of the High Plains aquifer, and the Mississippi Embayment (Fig. 3b). Responses in the mostly confined aquifers on the North Atlantic coast may be associated with municipal or energy production water demands varying with climate[34], and expanding agricultural production. Granger causality[35] results demonstrate the proposed relationship between precipitation, groundwater level change, and groundwater extraction available from Kansas; precipitation causes changes in rates of groundwater pumping ($p < 0.01$), and likewise groundwater pumping causes changes in groundwater levels in deep (>30 m) wells ($p < 0.05$). These analyses support the connection

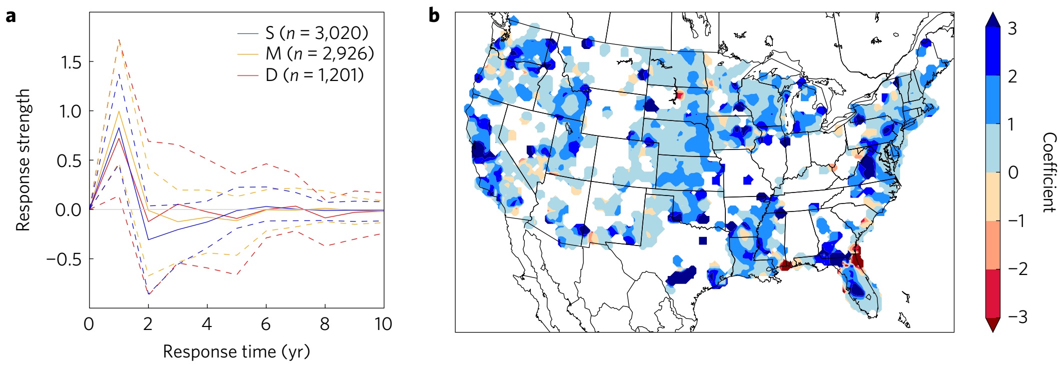

Figure 3 | Groundwater response to annual precipitation variability. a, Impulse response (precipitation anomaly on groundwater level change) using vector autoregression (VAR) results: mean (solid lines) and quartiles (dashed lines) shown for S wells (blue), M wells (yellow) and D wells (red). **b**, First VAR coefficient for all wells with stable VAR results.

between climate, pumping, and groundwater suggested by the VAR results.

Pumping for irrigation was previously shown to be comparable to or more influential for long-term groundwater trends than climate in central North America[36,37]. Their conclusions are likely to be conservative, because they do not consider the indirect interannual effects of climate on groundwater levels via changes in water demand; most notably in agricultural regions where climate influences crop water requirements. The direct effects of climate change influencing groundwater recharge rates[38] may be dominated by those associated with groundwater pumping changes for deep aquifers. The lack of groundwater pumping records is a critical barrier for directly estimating these effects.

Deep groundwater resources are often not formally considered in water balance models due to lack of data and a lack of understanding of the connection to climate and water use. They normally represent the 'slow' component of the hydrologic system, whereas river flow and shallow groundwater represent the 'fast' components. It appears that the nature of these dynamics may be changing by human pumping response to structured changes in precipitation over time. This also has implications for changes in the chemical composition of aquifer systems, through the induced migration of shallow groundwater to deeper aquifers and the ensuing mixing at timescales that may be relevant for geochemical changes. Recognizing the coupled human–natural system interactions, we must improve methods for simulating and validating deeper aquifer system dynamics as a critical part of the hydrologic cycle. Long-term monitoring of deep groundwater levels and chemistry, as well as of pumping and recharge, is critical for developing and applying such methods and understanding the spatio-temporal dynamics of these coupled systems. As seasonal to interannual climate predictability improves, there may be opportunities for improved integrated management of surface and ground waters, through tradable forward contracts between surface and groundwater users to improve the utilization of deeper aquifers for buffering persistent climate exigencies, including managed aquifer recharge in wet years.

Methods

Methods, including statements of data availability and any associated accession codes and references, are available in the online version of this paper.

Received 27 September 2016; accepted 20 December 2016; published online 23 January 2017

References

1. Döll, P. *et al*. Impact of water withdrawals from groundwater and surface water on continental water storage variations. *J. Geodyn.* **59–60,** 143–156 (2012).
2. Famiglietti, J. S. The global groundwater crisis. *Nat. Clim. Change* **4,** 945–948 (2014).
3. Maupin, M. *et al*. *Estimated Use of Water in the United States in 2010: USGS Circular 1405* (US Geological Survey, 2014).
4. Siebert, S. *et al*. Groundwater use for irrigation—a global inventory. *Hydrol. Earth Syst. Sci.* **14,** 1863–1880 (2010).
5. Scanlon, B. R. *et al*. Groundwater depletion and sustainability of irrigation in the US High Plains and Central Valley. *Proc. Natl Acad. Sci. USA* **109,** 9320–9325 (2012).
6. Konikow, L. F. *Groundwater Depletion in the United States (1900–2008)* Scientific Investigations Report 2013–5079 (US Geological Survey, 2013).
7. Scanlon, B. R., Reedy, R. C., Gates, J. B. & Gowda, P. H. Impact of agroecosystems on groundwater resources in the Central High Plains, USA. *Agric. Ecosyst. Environ.* **139,** 700–713 (2010).
8. Ho, M. *et al*. America's Water: agricultural water demands and the response of groundwater. *Geophys. Res. Lett.* **43,** 7546–7555 (2016).
9. Fan, Y., Li, H. & Miguez-Macho, G. Global patterns of groundwater table depth. *Science* **339,** 940–943 (2013).
10. USGS-NWIS *USGS Groundwater Levels for the Nation* (Accessed 2016).
11. Clark, B., Hart, R. & Gurdak, J. *Groundwater Availability of the Mississippi Embayment* Professional Paper 1785 (US Geological Survey, 2011).
12. *Farm and Ranch Irrigation Survey* (USDA, 2013).
13. Green, T. R. *et al*. Beneath the surface of global change: impacts of climate change on groundwater. *J. Hydrol.* **405,** 532–560 (2011).
14. Earman, S. & Dettinger, M. Potential impacts of climate change on groundwater resources—a global review. *J. Wat. Clim. Change* **2,** 213–229 (2011).
15. Whittemore, D. O., Butler, J. J. Jr & Wilson, B. B. Assessing the major drivers of water-level declines: new insights into the future of heavily stressed aquifers. *Hydrol. Sci. J.* **61,** 134–145 (2016).
16. Kuss, A. J. M. & Gurdak, J. J. Groundwater level response in U.S. principal aquifers to ENSO, NAO, PDO, and AMO. *J. Hydrol.* **519,** 1939–1952 (2014).
17. Taylor, R. *et al*. Ground water and climate change. *Nat. Clim. Change* **3,** 322–329 (2013).
18. Hanson, R. T. & Dettinger, M. D. Ground water/surface water responses to global climate simulations, Santa Clara–Calleguas Basin, Ventura, CA. *J. Am. Wat. Resour. Assoc.* **41,** 517–536 (2005).
19. Holman, I. P., Rivas-Casado, M., Bloomfield, J. P. & Gurdak, J. J. Identifying non-stationary groundwater level response to North Atlantic ocean-atmosphere teleconnection patterns using wavelet coherence. *Hydrogeol. J.* **19,** 1269–1278 (2011).
20. Bakker, M. & Nieber, J. L. Damping of sinusoidal surface flux fluctuations with soil depth. *Vadose Zone J.* **8,** 119–126 (2009).
21. Dickinson, J. E., Ferré, T. P. A., Bakker, M. & Crompton, B. A screening tool for delineating subregions of steady recharge within groundwater models. *Vadose Zone J.* http://dx.doi.org/10.2136/vzj2013.10.0184 (2014).
22. Chen, Z., Grasby, S. E. & Osadetz, K. G. Relation between climate variability and groundwater levels in the upper carbonate aquifer, southern Manitoba, Canada. *J. Hydrol.* **290,** 43–62 (2004).
23. Scanlon, B. R., Reedy, R. C., Stonestrom, D. A., Prudic, D. E. & Dennehy, K. F. Impact of land use and land cover change on groundwater recharge and quality in the southwestern US. *Glob. Change Biol.* **11,** 1577–1593 (2005).
24. Gurdak, J. J. *et al*. Climate variability controls on unsaturated water and chemical movement, High Plains Aquifer, USA. *Vadose Zone J.* **6,** 533–547 (2007).

25. Van Loon, A. F. *et al*. Drought in the anthropocene. *Nat. Geosci.* **9,** 89–91 (2016).
26. Condon, L. & Maxwell, R. Feedbacks between managed irrigation and water availability: diagnosing temporal and spatial patterns using an integrated hydrologic model. *Wat. Resour. Res.* **50,** 2600–2616 (2014).
27. Healy, R. W. & Cook, P. G. Using groundwater levels to estimate recharge. *Hydrogeol. J.* **10,** 91–109 (2002).
28. Sophocleous, M. On understanding and predicting groundwater response time. *Ground Water* **50,** 528–540 (2012).
29. Bredehoeft, J. D. Monitoring regional groundwater extraction: the problem. *Ground Water* **49,** 808–814 (2011).
30. Hanson, R. T., Dettinger, M. D. & Newhouse, M. W. Relations between climatic variability and hydrologic time series from four alluvial basins across the southwestern United States. *Hydrogeol. J.* **14,** 1122–1146 (2006).
31. *Climate Monitoring Teleconnections* (NOAA, 2015); http://www.ncdc.noaa.gov/teleconnections
32. Maurer, E., Wood, A., Adam, J., Lettenmaier, D. P. & Nijssen, B. A long-term hydrologically based dataset of land surface fluxes and states for the conterminous United States. *J. Clim.* **15,** 3237–3251 (2002).
33. *Kansas Irrigation Water Use* (Kansas Department of Agriculture, USGS, Kansas Water Office, 2013).
34. Akuoko-Asibey, A., Nkemdirim, L. C. & Draper, D. L. The impacts of climatic variables on seasonal water consumption in Calgary, Alberta. *Can. Wat. Resour. J.* **18,** 107–116 (1993).
35. Granger, C. Investigating causal relations by econometric models and cross-spectral methods. *Econometrica* **37,** 424–438 (1969).
36. Loáiciga, H. Climate change and ground water. *Ann. Assoc. Am. Geogr.* **93,** 37–41 (2003).
37. Ferguson, I. M. & Maxwell, R. M. Human impacts on terrestrial hydrology: climate change versus pumping and irrigation. *Environ. Res. Lett.* **7,** 044022 (2012).
38. Döll, P. Vulnerability to the impact of climate change on renewable groundwater resources: a global-scale assessment. *Environ. Res. Lett.* **4,** 035006 (2009).

Acknowledgements

Support for this work comes from NSF Water Sustainability and Climate Project #1360446, the Columbia Earth Institute Postdoctoral Fellowship Program, and the University of Chicago 1896 Pilot Project. We thank K. Mankoff for help with data collection and preprocessing. The data described in this paper are available from the USGS and NOAA websites.

Author contributions

T.A.R. and U.L. contributed to the analysis and writing of this article.

Additional information

Supplementary information is available in the online version of the paper. Reprints and permissions information is available online at www.nature.com/reprints. Correspondence and requests for materials should be addressed to T.A.R.

Competing financial interests

The authors declare no competing financial interests.

Methods

Data collection. Groundwater-use data reported by the US Geological Survey's National Water Use Information Program was used to identify regions of high groundwater extraction and areas with large rates of groundwater-supported irrigation (Supplementary Fig. 1). Groundwater levels are reported by the US Geological Survey (USGS, NWIS). Groundwater level measurements are taken from USGS monitoring wells, agency or state operated wells, and domestic wells (Supplementary Fig. 2A). We used groundwater level records from 15,148 wells with a minimum of 100 observations during the study period, 1940 to 2015. Additional requirements were applied for generating record subsets for each analysis. Trend analysis required wells to have at least ten years of records. The frequency analysis required nearly continuous (defined below) records from 1963 to 2004. The VAR analysis was applied on continuous data series longer than ten years.

Groundwater level observations were taken at varying frequencies, and were rarely continuous over the entire study period. The number of observation wells decreases exponentially with increasing depth (Supplementary Fig. 2B). Wells included in this study ranged between 0 and 3,150 m deep. Groundwater wells were classified into the three depth analysis groups: S (<30 m), M (30–150 m), and D (>150 m), where S is referred to as 'shallow' and M and D are together referred to as 'deep' wells. Note that the well depth is the depth of the borehole or installed well, and is different than the measured depth of groundwater.

Groundwater level measurements are relatively well distributed across the country, with notable exceptions in the eastern-central part of the country (Supplementary Fig. 2A). Regions with the largest groundwater extraction tend to be most densely monitored (Supplementary Figs 1 and 2A). Agriculture is a major user of groundwater; note the high groundwater use in agricultural regions such as the Central Valley of California, the High Plains, and the Mississippi Embayment aquifers (Supplementary Fig. 2B).

Analysis. *Groundwater depth.* The annual (water year: 1 October to 30 September) average depth to groundwater measured between 1990 and 2015 (inclusion) was plotted for all wells deeper than 30 m (groups M and D). There were 8,173 wells in these groups with measurements between 1990 and 2015. Data from 1990 and later were selected to represent relatively recent groundwater levels and include a broad spatial set of wells. Average depth values were gridded at 20 km resolution and then interpolated using Barnes analysis, with a region of interest set to 40 km (Fig. 1).

Barnes analysis (also referred to as Barnes interpolation) is an interpolation method which uses two steps: first, generate a weighted spatial average using the sum of Gaussian decay functions around each measurement point, then improve the initial estimate by adding the calculated error surface (based on the latest surface estimate and the original measurements) and repeat until a convergence factor is met. The resulting national maps of groundwater depth and groundwater trends (discussed in the next section) were compared to alternative interpolation methods including inverse distance weighting (IDW) and kriging. The assumption of stationarity of the variograms of kriging at the national scale is probably untenable, and although this could be overcome using nonstationary variograms, we preferred a simpler approach for our purpose here. When comparing the two methods, we found the regions where the kriged probability was high (>90%) showed generally the same values as seen in the Barnes analysis. Barnes analysis was selected because it offers a weighted spatial analysis, and includes error analysis to refine the result—providing better results than IDW.

Average groundwater trend. Annual (water year) average groundwater level depth trends were calculated for each well with more than ten annual years of record over the study time period, 1940 to 2015. For every well, the presence and statistical significance of monotonic groundwater elevation trends over the study period was evaluated using the Mann–Kendall test, a common method for identifying trends in hydrologic time series data[39]. We consider groundwater records with a p value <0.1 in rejection of the null hypothesis of no trend to be significant ($\tau = 0$).

For all wells, the linear slope of the time trend of groundwater level was calculated using the Theil–Sen method[40]. This is a trend estimator used in conjunction with the Mann–Kendall test, and is robust to nonlinearity and outliers. Outliers in field-collected groundwater level records may be caused by a number of factors, including human error or measuring at a time when the groundwater level was strongly impacted by active pumping. Average slope values are gridded at 20 km resolution and then interpolated using the Barnes method, with a region of interest set to 70 km.

The interpolated map of groundwater level trends for shallow and deep wells is shown in Fig. 2. Of the shallow (<30 m) wells, there were 3,441 wells with significant ($p < 0.1$) trends in groundwater level (54% of analysed shallow wells). There were 5,743 deep (>30 m) wells with significant ($p < 0.1$) trends in groundwater level (74% of analysed deep wells). Large regions with generally contiguous deep groundwater declines include the central and southern High Plains Aquifer, the Mississippi Embayment Aquifer System, the Southwest and central–western United States, and the mid-Atlantic coast. Rises in deep groundwater, as seen in parts of California and Nevada, may be attributed to changes in pumping regulations and groundwater recharge projects.

Groundwater elevation and climate indices. Groundwater and climate connections were assessed using bivariate wavelet analysis using the Morlet wavelet function. The study period for the frequency analysis was 1963 to 2004; it was shorter than the full study period to increase the number of wells with continuous records. Wells meeting the following three criteria were included in the frequency analysis: no missing data in the first or last year of the study period; not more than four missing records in total; and not more than one consecutive missing record (Supplementary Fig. 3). Gaps in these records were interpolated using splines.

A wavelet cluster analysis was performed using Ward's agglomerative hierarchical clustering[41] applied to the global wavelet spectrum[42] associated with each well time series. The method identified clusters that represent common frequency-domain behaviour across the set of wells considered. The number of clusters used was selected based on parsimony and the silhouette coefficient[43]. The S, M and D categories had 3, 4 and 5 clusters, respectively (Supplementary Fig. 4). The first principal component (PC1) for the well time series in each cluster was then used with each climate index (ENSO, NAO and PDO) time series to compute the wavelet coherence and the wavelet cross-spectrum[42] (for example, Supplementary Fig. 5). We provide an example of the wavelet of PC1 for the M depth wells (Supplementary Fig. 5A) which shows high power at 4- to 6-year periods from the early 1970s to early 1980s, and for the >11-year period throughout the study period. For this cluster, the wavelet coherence power is greatest overall for ENSO (Supplementary Fig. 5B,E); however, coherence is also observed with both NAO and PDO. Results show varying coherence by cluster between groundwater levels and climate indices for all depths and indices.

Wavelet coherence results were evaluated to assess correlations between groundwater and climate for the three well depth categories (S, M and D) over the study period. Periods of coherence with high power and confidence were identified over eight equal time intervals between 1963 and 2004. The percentage of high-coherence spectrum power periods with each climate index was determined for each well depth category (Supplementary Table 1). For the shallow wells (S), a majority of periods with strong coherence to the climate indices occurred with ENSO. The M wells had equal total coherence to ENSO and PDO. The D wells had the most coherence with ENSO, followed by NAO.

High power in the wavelet coherence spectrum between groundwater and one or more climate indices was recorded for eight time intervals between 1963 and 2004 (Supplementary Table 2). All three depths showed coherence at the longest (>11 yr) periods between 1963 and 2004, and M and D wells also showed consistent coherence at the 4- to 6-year periods. Overall, the number of intervals with coherence to at least one climate pattern increased with well depth. The number of times an individual well cluster had high coherence to a climate index was not compared across depths due to the different numbers of clusters in each depth category. Cross-wavelet phase difference results indicated that the climate signal led the groundwater signal in most cases, with some variability for shorter periods. When the phase is near half the period length, it becomes challenging to detect the difference between leading and lagging variables.

Groundwater elevation, local precipitation, and pumping. A vector autoregression (VAR) process for multivariate time series data was used to model the relationship between the local annual precipitation anomaly and annual groundwater level changes. The basic p-lag VAR model is shown in equation (1) and is solved using the ordinary least squares method[44]. The subset of the model for annual groundwater level change based on lagged groundwater level change and precipitation values is given in equation (3):

$$\mathbf{Y}_t = A_1\mathbf{Y}_{t-1} + A_2\mathbf{Y}_{t-2} + \cdots + A_n\mathbf{Y}_{t-n} + \boldsymbol{\varepsilon}_t \tag{1}$$

$$Y_{1t} = \alpha_{11}^1 y_{1t-1} + \alpha_{12}^1 y_{2t-1} + \cdots + \alpha_{11}^n y_{1t-n} + \alpha_{12}^n y_{2t-n} + \varepsilon_{1t} \tag{2}$$

$$Y_{2t} = \alpha_{21}^1 y_{1t-1} + \alpha_{22}^1 y_{2t-1} + \cdots + \alpha_{21}^n y_{1t-n} + \alpha_{22}^n y_{2t-n} + \varepsilon_{2t} \tag{3}$$

where $\mathbf{Y}_t$ is a vector of j time series variables, t is time, A_n is a $(j \times j)$ coefficient matrix and $\boldsymbol{\varepsilon}_t$ is a constant. In the two-variable case with precipitation anomaly and change in groundwater level, $j = 2$, where Y_1 = annual precipitation anomaly and Y_2 = annual groundwater level change.

Change in groundwater level is calculated as the change in groundwater elevation between two subsequent years. If one (or both) of the years in the record do not have groundwater observations then NaN is assigned. The time series of annual groundwater level changes is then used in the analysis. County precipitation anomaly data were used for each corresponding well. The models for Y_{2t} were fitted using up to a 5-year lag using wells records of at least ten consecutive years (containing no NaN values). Y_{1t} was not modelled, but provided data so that the impulse response of Y_2 given Y_1 could be computed.

For results with stable VAR coefficients, a moving average (MA) representation of the VAR process was used to calculate the impulse response of precipitation on annual groundwater level change over a 10-period (yr) duration. The response in groundwater level change is estimated for a unit impulse in precipitation. The impulse responses were calculated for wells in three depth categories (S, M and D). The response strengths at each well were spatially interpolated using the Barnes method and plotted separately for each well depth group (Fig. 3a). The quartiles of the distribution (25th and 75th percentiles) are shown in dashed lines bracketing the median values. Results indicate for all depths that the strongest positive response occurs within one year from the impulse. On the basis of the results showing the strongest impulse response within one year, the first coefficient (α^1_{21}) for groundwater level change (Y_2) as a function of precipitation anomaly (y_1) was selected for plotting. The first coefficients for all wells were gridded at a 25 km resolution, and interpolated using the Barnes method with a 60 km region of interest (Fig. 3b).

A Granger causality test was used to determine the significance of the causal relationship between precipitation anomaly and groundwater level change[35,44]. Granger causality is defined where $\sigma^2(x|\mathbf{F}_1) > \sigma^2(x|\mathbf{F}_2)$, where

$$\mathbf{F}_1 = x_t, x_{t-1}, x_{t-2}, \ldots \quad (4)$$

$$\mathbf{F}_2 = x_t, y_t, x_{t-1}, y_{t-1}, x_{t-2}, y_{t-2}, \ldots \quad (5)$$

demonstrating that the prediction of x is improved if y is included. The causal model where y_t is causing x_t is defined as

$$x_t = \sum_{j=1}^{m} a_j x_{t-j} + \sum_{j=1}^{m} b_j y_{t-j} + \varepsilon_t \quad (6)$$

where ε_t is an uncorrelated white noise series, and we assume that b_j is not zero[35]. We applied this test to the groundwater level changes (x) and annual precipitation (y). Results indicated that the models for 73% of the individual wells found precipitation was Granger-causal for predicting groundwater level change ($p < 0.1$).

Following the finding of the annual response between precipitation and groundwater in deep aquifers, the relationship between precipitation and pumping was investigated. Pumping records are not typically published, and generally exist only for individual wells[24], sparse temporal frequencies (for example, estimates every five years (USGS Water Use)), or short historical periods. We obtained irrigation (groundwater pumping) data for eight groundwater management districts in the State of Kansas (USA) from 2007 to 2013, inclusive. The data irrigation districts were grouped into western, central, and eastern Kansas, with a majority of groundwater use occurring in the drier western and central regions.

The causality of precipitation on pumping—and pumping on groundwater level change—was assessed in each of three spatial areas (western, central and eastern) of Kansas. Precipitation anomalies and pumping anomalies were pooled for all climate stations across each region of the state. Results indicate that precipitation Granger causes[35] pumping variability ($p < 0.01$) in all three regions. Likewise, pumping anomalies and groundwater level change anomalies were pooled for all wells within each of the three regions, respectively. Results indicate that pumping Granger causes groundwater level change ($p < 0.05$).

In addition to the causality test, we used the Theil–Sen method to calculate the linear slopes of the pumping anomalies versus precipitation anomalies at individual weather stations, and pumping anomalies versus groundwater level change at individual wells, respectively. The results suggest a correlation between precipitation and pumping, and likewise between pumping and groundwater level change. For all three regions of Kansas, a large majority of the precipitation stations show negative correlations with pumping, suggesting pumping increases during drier years (Supplementary Fig. 6). The difference in the magnitudes of the slopes appears to increase from West to East across the state, also following the precipitation gradient from lowest to highest. The sensitivity of water demand and pumping to precipitation variability may be a function of total precipitation, and could be worth further exploration.

Groundwater level changes at individual wells within each of the groundwater management regions were compared to pumping anomalies, and the slopes were averaged for each county (Supplementary Fig. 7). The results show a majority of positive slopes, where positive slope indicates a higher irrigation anomaly corresponding to a greater decline in groundwater. Some of the counties with negative correlations between pumping and groundwater change may be due to surface water contributions. The state report notes that irrigation totals do not include surface water withdrawn under ditch irrigation rights in the southwest[33].

The correlation coefficients for both sets of analyses indicate that $>60\%$ of the sites have $R > 0.5$, with approximately 20% of the sites having $R > 0.8$ (Supplementary Fig. 8). Results from the exploratory analysis and the causality test confirm a potential relationship between precipitation and pumping, which could reasonably explain the changes in groundwater level observed in deep and poorly connected aquifers. The limited historical data preclude us from assessing the significance of these observations, and further emphasize the need for groundwater extraction records to better understand climate–groundwater dynamics.

Code availability. The codes used in this study are available from the corresponding author on request.

Data availability. The groundwater level, climate, and irrigation data that support the findings of this study are publicly available from the sources listed in the article[10,31–33]. The data sets are available from the corresponding author upon request.

References

39. Hirsch, R. M., Slack, J. R. & US Geological, A nonparametric trend test for seasonal data with serial dependence. *Wat. Resour. Res.* **20,** 727–732 (1984).
40. Helsel, D. & Hirsch, R. *Statistical Methods in Water Resources* (Elsevier, 1992).
41. Murtagh, F. & Legendre, P. Ward's hierarchical agglomerative clustering method: which algorithms implement ward's criterion? *J. Classif.* **31,** 274–295 (2014).
42. Torrence, C. & Compo, G. P. A practical guide to wavelet analysis. *Bull. Am. Meteorol. Soc.* **79,** 61–78 (1998).
43. Rousseeuw, P. Silhouettes: a graphical aid to the interpretation and validation of cluster analysis. *J. Comput. Appl. Math.* **20,** 53–65 (1987).
44. Lütkepohl, H. *New Introduction to Multiple Time Series Analysis* (Springer, 2005).